

COMPACT SPLIT RING SIR BANDPASS FILTERS WITH DUAL AND TRI-BAND

J.-K. Xiao^{1,2,*} and W.-J. Zhu³

¹School of Electronical & mechanical Engineering, Xidian University, Xi'an 710071, China

²State Key Laboratory of Millimeter Waves, Nanjing 210096, China

³School of Computer and Information, Hohai University, Changzhou 213022, China

Abstract—Multi-band microwave filters are important for multifunctional and miniaturization requirement of portable communication equipment. In this paper, tri-section split ring stepped-impedance resonator is analyzed, and new compact dual-band and tri-band bandpass filters are proposed by using split ring stepped-impedance resonators, and the designs are demonstrated by measurement. The new dual-band filters operate at about 2.4 and 5.5 GHz which meet IEEE 802.11 application requirements, and the new tri-band filters operate at about 2.4–2.6, 3.3–3.6 and 5.2–5.6 GHz, and filter sizes are greatly reduced compared with relative reports. The designed filters have advantages of compact and miniature structures, low passband insertion losses and good frequency selectivity, all these have prospect to be applied in wireless communication systems.

1. INTRODUCTION

In many communication related applications, it is important to keep RF filter structures to a minimum size and weight, and filter performances to low passband insertion losses, high frequency selectivity, and flat group delay within the passband. Currently, with the rapid development of modern wireless communications, bandpass filters with dual-band [1–7] and tri-band [8–10] even quad-band [11] operation become more and more important in communication

Received 28 September 2011, Accepted 2 November 2011, Scheduled 9 November 2011

* Corresponding author: Jian-Kang Xiao (xiaojk@lzu.edu.cn).

systems for the multifunctional and miniaturization requirement of portable equipment. The traditional microstrip parallel-coupled half-wavelength resonator bandpass filters have narrow stopband between the fundamental response and the first spurious response, so the stepped-impedance resonator (SIR) [6–8] was presented in the past years not only to restrain the spurious responses, but also to shorten the resonator size. SIR also can be used to design tri-band even multi-band filters for tuning the higher order resonant modes conveniently. The deficiency of this kind of resonator is its resonant frequencies are dependent, and transmission zeros are difficult to implement, especially for the fundamental SIR.

Commonly, there are the following methods for dual- and multi-band filter design: the first is using cascade resonators including the stepped impedance resonator [7, 8, 12], the second is using two sets of different resonators with two-path coupling [3], the third is using new resonator [2], and the fourth is using dual-mode [1, 2] or multi-mode resonator. In this paper, split ring tri and quad-section SIR bandpass filters with dual-band operation are presented, and compared with dual-band filters with two sets of different resonators or two paths coupling, the new filter sizes are greatly reduced. The proposed SIR dual-band filters have size reduction of about 75% and 77% compared with [2] and [12], respectively. Split ring SIR bandpass filters with tri-band operation by using two sets of different resonators with two-path coupling are also proposed, and which have size reduction of about 81% and 68.3% compared with [8] and [12], respectively. The new designs are demonstrated by experiment.

2. ANALYSIS OF SPLIT RING MULTI-SECTION SIR

Fundamental half wavelength microstrip stepped-impedance resonator is formed by joining together microstrip transmission lines with different characteristic impedance of Z_1 and Z_2 , and the corresponding electric lengths are θ_1 and θ_2 , respectively, as Fig. 1(a) shows. Compared with the fundamental half wavelength SIR, tri-section SIR as shown in Figs. 1(b) and (c) has more parameters for controlling, and which can get more desired band or better harmonics suppression, where, characteristic impedance of a tri-section SIR are Z_1 , Z_2 and Z_3 , and the corresponding electric length are θ_1 , θ_2 and θ_3 , respectively. For the split ring tri-section SIR as shown in Fig. 1(c), according to the relative procedure in [13], if $k_1 = Z_3/Z_2$, $k_2 = Z_2/Z_1$, and $\theta_1 = \theta_2 = \theta_3 = \theta$, θ can be calculated as $\theta = \tan^{-1} \left(\sqrt{\frac{k_1 k_2}{k_1 + k_2 + 1}} \right)$, and

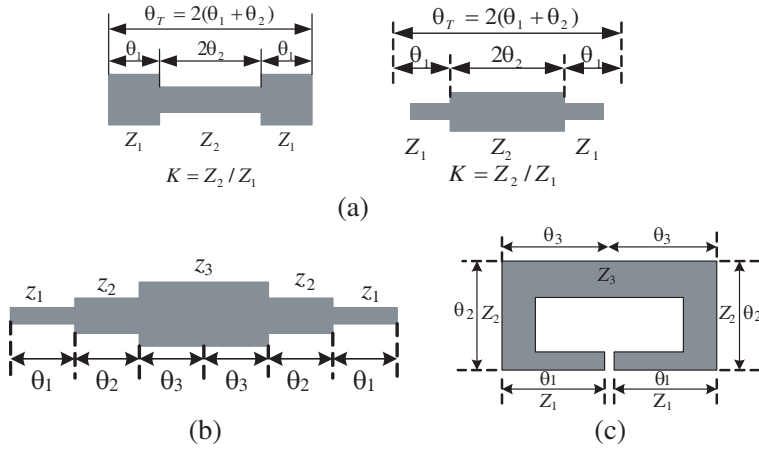


Figure 1. SIR structures. (a) Fundamental half-wavelength SIR. (b) Fundamental tri-section SIR. (c) Split ring tri-section SIR.

the total electric length can be got as

$$\theta_T = 6 \tan^{-1} \left(\sqrt{\frac{k_1 k_2}{k_1 + k_2 + 1}} \right). \quad (1)$$

And the resonant frequency of the first spurious (the second passband) can be got as

$$f_{s1} = \frac{\theta_{s1}}{\theta} f_0. \quad (2)$$

where, f_0 is the fundamental resonance (the first passband) and θ_{s1} can be expressed as

$$\theta_{s1} = \tan^{-1} \sqrt{\frac{(k_1 + 1)^2(k_2 + 1) + k_2^2 k_1}{k_2^2 + k_1 k_2 + k_2}}. \quad (3)$$

Figure 2 gives the tri-section split ring SIR and their equivalent transmission line model. In the research we find split ring SIR shown in Fig. 2(c) has more resonance than the structure shown in Fig. 2(a) for the split ring SIR with inner coupling is more easy introducing higher order modes. With the assistance of Matlab, computed relationship curves of f_{s1}/f_0 versus k_2 , and θ_T versus k_2 for the split ring tri-section SIR are shown in Fig. 3 and Fig. 4, respectively. It shows the value of f_{s1}/f_0 decreases with k_2 increasing, while, the total electric length increases with k_2 increasing, and both exist various k_1 and k_2 . Table 1 shows the calculated concrete values of f_{s1}/f_0 and θ_T for the split ring tri-section SIR, and it can be seen for $k_1 \leq 1$ and $k_2 < 1$, the second

Table 1. Calculated results of f_{s1}/f_0 and θ_T for the split ring tri-section SIR.

| k_1 and k_2 values | f_{s1}/f_0 | θ_T |
|------------------------|--------------|------------|
| $k_1 = 0.6, k_2 = 0.4$ | 3.5 | 114.6° |
| $k_1 = 1.0, k_2 = 0.4$ | 3.12 | 133.2° |
| $k_1 = 1.0, k_2 = 0.8$ | 2.25 | 168.8° |
| $k_1 = 0.6, k_2 = 0.6$ | 2.86 | 132.1° |

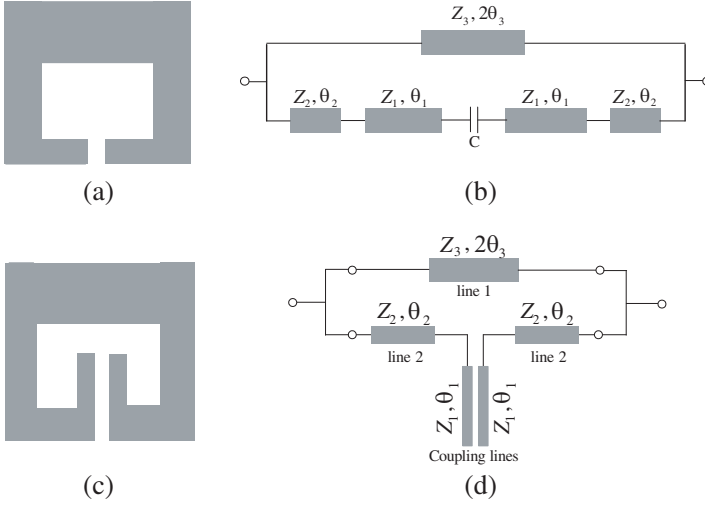


Figure 2. Tri-section split ring SIR. (a) Tri-section split ring SIR. (b) Equivalent circuit of (a). (c) Tri-section SIR with inner coupling. (d) Equivalent circuit of (c).

passband is always located above $2f_0$. The external quality factor of the split ring tri-section SIR will be discussed in the following part.

For the split ring quad-section SIR, resonant condition can be got on the basis of transmission line theory and synthesizing the equivalent input impedance of each step as

$$\begin{aligned}
 & 1 - \frac{Z_1}{Z_2} \operatorname{tg} \theta_1 \operatorname{tg} \theta_2 - \frac{Z_1}{Z_3} \operatorname{tg} \theta_1 \operatorname{tg} \theta_3 - \frac{Z_2}{Z_3} \operatorname{tg} \theta_2 \operatorname{tg} \theta_3 - \frac{Z_1}{Z_4} \operatorname{tg} \theta_1 \operatorname{tg} \theta_4 \\
 & - \frac{Z_2}{Z_4} \operatorname{tg} \theta_2 \operatorname{tg} \theta_4 - \frac{Z_3}{Z_4} \operatorname{tg} \theta_3 \operatorname{tg} \theta_4 + \frac{Z_1 Z_3}{Z_2 Z_4} \operatorname{tg} \theta_1 \operatorname{tg} \theta_2 \operatorname{tg} \theta_3 \operatorname{tg} \theta_4 = 0 \quad (4)
 \end{aligned}$$

where, characteristic impedance of the quad-section SIR are $Z_1, Z_2,$

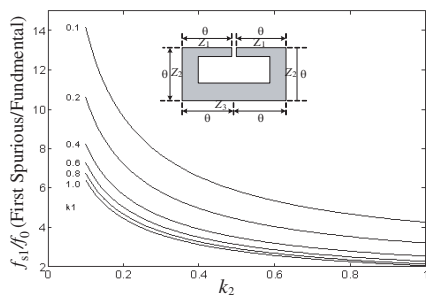


Figure 3. Relationships of f_{s1}/f_0 versus k_2 for the split ring tri-section SIR.

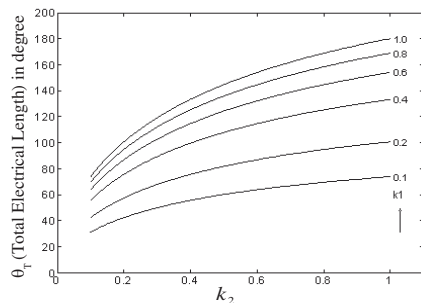


Figure 4. Relationships of θ_T versus k_2 for the split ring tri-section SIR.

Z_3 and Z_4 , and the corresponding electric length are θ_1 , θ_2 , θ_3 and θ_4 , respectively.

3. NEW DUAL-BAND BANDPASS FILTER

In recent years, in exploring advanced dual-band wireless systems, filters with dual-band operation for RF devices have become quite popular. It is easy to control the second passband by adjusting the impedance ratio and electric lengths of SIR. By properly selecting the relevant impedance or strip width ratio, the dual-band filters using stepped-impedance resonators can be created. Here, simple and compact tri-section and quad-section split ring SIR is used to get dual-band operation. All of the filters are designed on ceramic substrates with dielectric constant of 10.2 and thickness of 1.27 mm, and I/O feed lines are microstrip lines with characteristic impedance of 50 Ω . Presented dual-band bandpass filters with tri-section split ring SIR using 1-path coupling are shown in Fig. 5, where, for the filter topology 1 and topology 2, $a = 13$ mm, $b = 1.8$ mm, $d = 6.4$ mm, $e = 0.75$ mm, $f = 0.5$ mm, $g = 4$ mm. The external quality factor of a single resonator may be expressed as $Q_{ei} = f_{0i}/\Delta f_{3dB}$, where, Q_{ei} is the external quality factor of the i -th passband, and f_{0i} and Δf_{3dB} are the i -th resonant frequency and the corresponding 3-dB bandwidth of the resonator, when it is externally excited alone. Calculated results of external quality factor Q_e versus feeding position t for a split ring tri-section SIR are shown in Fig. 6, and it can be seen that this SIR has adequate external quality factor, for the first band, $Q_e > 85$, and for the second band $Q_e > 40$. Simulated frequency responses of the designed dual-band filters are plotted in Fig. 7, and it shows for the

first passband, filter 1 and filter 2 nearly have the same operation of 2.43 GHz, while, for the second passband, filter 1 and 2 operate at 5.32 GHz and 5.26 GHz, respectively, and the filter passband insertion loss is no more than 1 dB. Filter 1 has wider passband bandwidth compared with filter 2 for this structure has stronger coupling with feed line, and which introduces more energy exchange. For filter 1 and 2, the operation frequency of the dual-passband and 3 dB bandwidth of the first passband decrease with parameter a and g increasing, while, the operation frequency of the dual-passband and 3 dB bandwidth of the first passband increase with parameter e increasing.

Designed dual-band bandpass filters using split ring quad-section SIR with inner coupling are shown in Fig. 8. Equivalent circuit and transmission line model of the designed filter are plotted in Figs. 8(c) and (d), respectively. Where, the filter geometric dimensions are $a = 11.2$ mm, $b = 1.5$ mm, $c = 0.75$ mm, $d = 0.5$ mm, $e = 4$ mm, $f = 5.5$ mm, $s = 0.3$ mm, $t = 1.5$ mm. The dual-band are determined

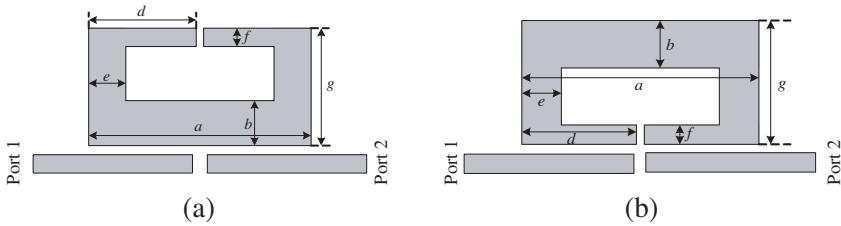


Figure 5. Dual-band SIR bandpass filters with 1-path coupling. (a) Filter 1. (b) Filter 2.

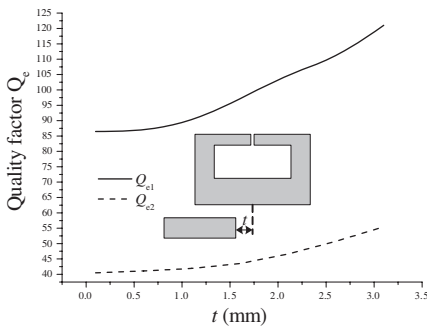


Figure 6. Calculated curves of external quality factor Q_e versus feeding position t .

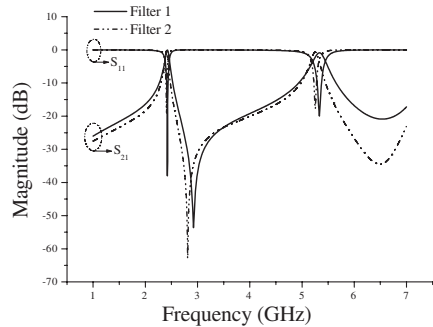


Figure 7. Simulated filter frequency responses comparison.

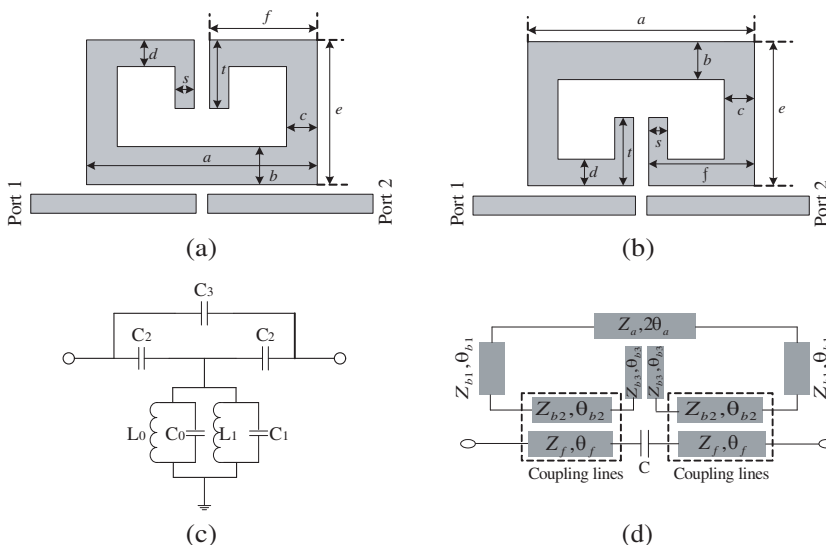


Figure 8. Dual-band bandpass filters using quad-section SIR with inner coupling. (a) Filter 3. (b) Filter 4. (c) Equivalent circuit. (d) Transmission line model of filter 4.

by resonances of L_0C_0 and L_1C_1 , I/O feed line is expressed as C_2 , and the coupling between input and output feed lines is denoted as C_3 . Characteristic impedance of each part for the quad-section SIR are $Z_a = 44.9 \Omega$, $Z_{b1} = 61.6 \Omega$, $Z_{b2} = 71.7 \Omega$, $Z_{b3} = 84.6 \Omega$ and $Z_f = 50 \Omega$. External quality factor of the split ring quad-section SIR with dual-resonance can be calculated as $Q_{e1} = 96.2$ and $Q_{e2} = 30.2$ when the feeding position $t = 0.1$ mm. Simulated frequency responses of filter 3 and filter 4 are plotted in Fig. 9, and it can be seen that for the first passband, the bandwidth of filter 3 is wider than that of filter 4, and for the second passband, they nearly have the same bandwidth. This is not only for the same reason as the above analysis but also for the inner coupling structure enhances energy coupling. For filter 3, it shows the dual-band operate at 2.4 GHz and 5.48 GHz with passband insertion loss of no more than 0.8 dB. Filter 4 has similar performance with filter 3. Simulated frequency responses comparison of filter 3 and 1 which with and without SIR inner coupling are plotted in Fig. 10, and it shows the two filters nearly have the same operation frequency for the first band. In the research, we find filter 3 which with inner coupling has a circuit size reduction of about 22% compared to the filter without inner coupling when the two filters have the same operation frequency of 2.4 GHz.

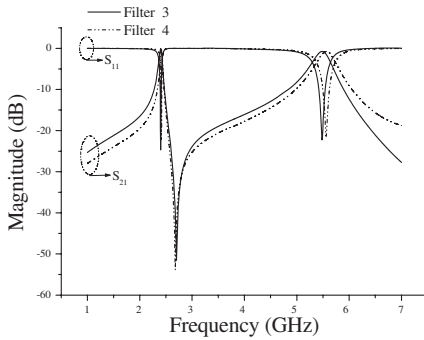


Figure 9. Simulated filter frequency responses.

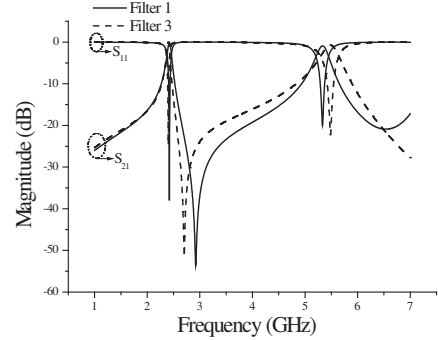


Figure 10. Simulated frequency responses comparison of filter 1 and 3.

4. NEW TRI-BAND BANDPASS FILTER

Tri-band bandpass filters are paid much attention for the multifunctional requirement of portable equipment. For a tri-band filter implementation, two-path coupling is introduced, and the filters are designed on the same material as the dual-band ones. Topologies of the proposed tri-band bandpass filters using assembled tri-section SIRs are plotted in Fig. 11, and Fig. 11(c) shows the filter coupling structure. Filter 5 and 6 have the same coupling method, and for the top tri-section SIR, it is identical to the assembled operation of a single resonator 1 and 2, respectively, while, the bottom tri-section SIR with a smaller size is denoted by resonator 3. For filter 5, physical parameters are as follows: $a = 11.5$ mm, $b = 1.8$ mm, $d = 6.4$ mm, $e = 0.75$ mm, $f = 0.5$ mm, $g = 4$ mm, $l = 10$ mm, $h = 4$ mm, $s = 4.9$ mm, $w = 1$ mm, $q = 0.5$ mm, and for filter 6, $a = 11$ mm, $b = 1.8$ mm, $d = 6.4$ mm, $e = 1$ mm, $f = 0.5$ mm, $g = 4$ mm, $l = 9$ mm, $h = 2.3$ mm, $s = 4.4$ mm, $w = 1$ mm, $q = 0.5$ mm. Simulated frequency responses of the proposed filters are shown in Fig. 12, and it can be seen that filter 5 operates at 2.4 GHz, 3.34 GHz, and 5.33 GHz with relative bandwidth of 5.86%, 4.5%, and 2.6%, respectively, while, filter 6 has the similar performances except for a higher operation frequency of the second band and a wider bandwidth of the third band. Both filters have passband insertion losses of no more than 1.7 dB. The first and the third passbands are implemented by coupling path 2, while, the second passband is implemented by path 1, and the tri-band bandpass filter is got by assembling path 1 and 2 together. In order to verify the design, a split ring SIR tri-band bandpass filter as shown in Fig. 11(b) is fabricated

and tested, and the fabrication and measurement are shown in Fig. 13. The measured results are got by Agilent E5071C vector network analyzer, and it shows the measurement is similar to the simulation. The measured filter performances and comparison with relative references are shown in Table 2, and it shows our design has better performances and smaller circuit size. The discrepancy of simulation and measurement is due to the simulation precision and fabrication uncertainty.

Tri-band bandpass filters using split ring SIR with inner coupling are also proposed, as shown in Fig. 14, and the two-path coupling structure is shown in Fig. 14(c). Where, filter 7 is assembled by a tri-section SIR and a quad-section SIR, while, filter 8 is assembled by quad-section SIRs with different size. Physical dimensions of the filters are as follows: for filter 7, $a = 9.2$ mm, $b = 1.5$ mm, $c = 1$ mm, $d = 0.5$ mm, $f = 5.5$ mm, $g = 4$ mm, $e = 0.3$ mm, $t = 1.5$ mm, $h = 4$ mm, $s = 4.9$ mm, $w = 1$ mm, $p = 0.2$ mm, $q = 0.5$ mm. For filter 8, $a = 9.2$ mm, $b = 1.5$ mm, $c = 1$ mm, $d = 0.5$ mm, $f = 5.5$ mm, $g = 3.6$ mm, $e_1 = 0.3$ mm, $e_2 = 0.2$ mm, $t_1 = 1.5$ mm, $t_2 = 1$ mm,

Table 2. Measurement comparison.

| | Literature [8] | Literature [12] | This paper |
|---------------------------------------|----------------|-----------------|--|
| Measured center frequency (GHz) | 1.0, 2.4, 3.6 | 2.3, 3.7, 5.3 | Filter 6: 2.4, 3.6, 5.2 Filter 8: 2.6, 3.5, 5.6 |
| Measured passband insertion loss (dB) | 2.0, 1.9, 1.7 | 2.5, 1.9, 2.9 | Filter 6: 2.5, 1.8, 0.8 Filter 8: 1.6, 2.1, 1.5 |
| Transmission zeros | No | 4 | 3–4 |
| Circuit size (mm ²) | 40 × 40 | 54.1 × 22.9 | Filter 6: 30 × 10 Filter 8: 30 × 10 |

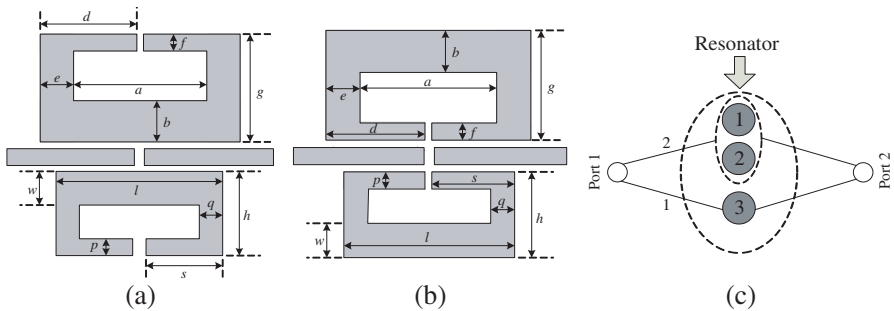


Figure 11. Tri-band SIR bandpass filters with two-path coupling. (a) Filter 5. (b) Filter 6. (c) Coupling structure.

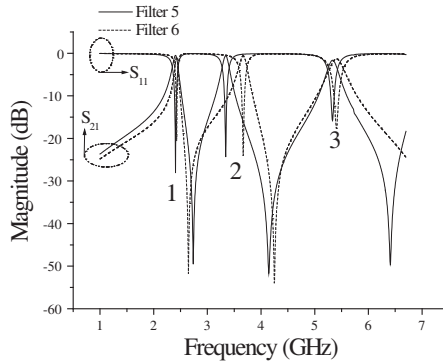


Figure 12. Simulated frequency responses of the tri-band filter.

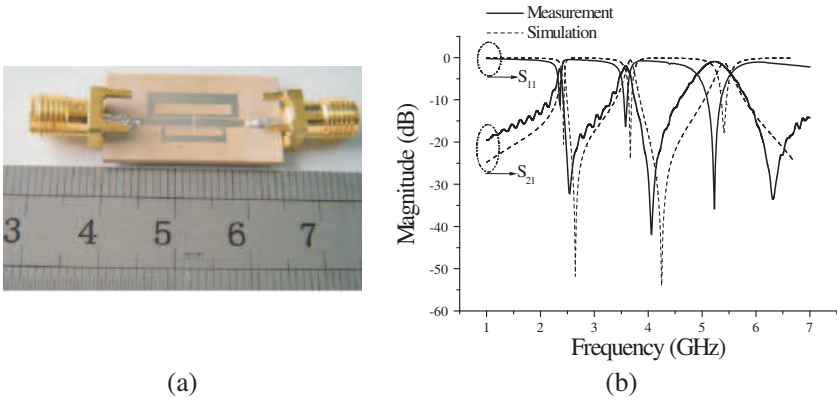


Figure 13. Fabricated hardware and measurement. (a) Photograph of the hardware. (b) Measurement and simulation comparison.

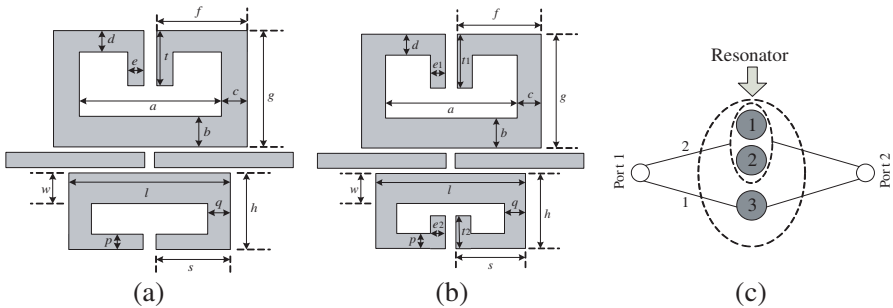


Figure 14. Tri-band bandpass filters with two-path coupling by using quad-section SIR with inner coupling. (a) Filter 7. (b) Filter 8. (c) Coupling structure.

$h = 2.5$ mm, $s = 4.2$ mm, $w = 1$ mm, $p = 0.2$ mm, $q = 0.5$ mm. Simulated filter frequency responses are plotted in Fig. 15, and it can be seen that filter 7 operates at 2.43, 3.32 and 5.6 GHz with passband insertion losses of no more than 1.4 dB. It also shows that filter 8 has higher operation frequencies than filter 7 for the first two bands, and the two kinds of filters have similar performances. Filter 8 is fabricated with 30×10 mm² and measured, as shown in Fig. 16, and the measured results agree with the simulation. The top SIR introduces passband 1 and 3 with coupling path 2, and the bottom SIR introduces passband 2 with coupling path 1. The measured filter operation frequency and passband insertion loss are shown in Table 2.

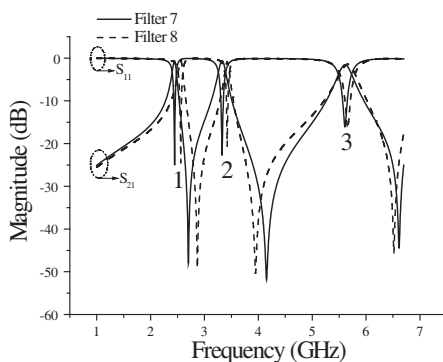


Figure 15. Simulated frequency responses of the tri-band filter.

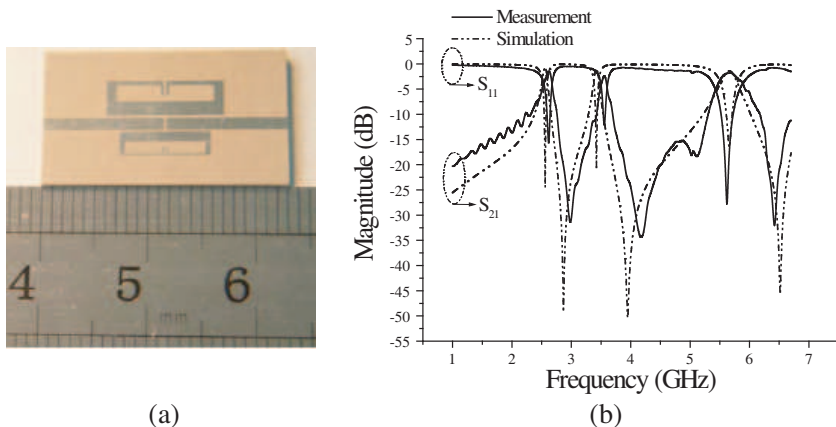


Figure 16. Fabricated hardware and measurement. (a) Photograph of the hardware. (b) Measurement and simulation comparison.

5. CONCLUSIONS

Tri-section split ring stepped impedance resonator is analyzed, and the advanced dual-band and tri-band bandpass filters using split ring SIR which suit to wireless communication applications are proposed. The sizes of the filters have been significantly reduced, and two filter prototypes are fabricated, and their measured results demonstrate the correctness of the design. Results indicate that the proposed filters have properties of compact and miniature sizes, low passband insertion losses and high frequency selectivity.

ACKNOWLEDGMENT

This work was supported in part by Research Fund of China State Key Laboratory of Millimeter Waves (K201107), and Specialized Research Fund for the Doctoral Program of Higher Education (200805611077).

REFERENCES

1. Luo, S., L. Zhu, and S. Sun, "A dual-band ring-resonator bandpass filter based on two pairs of degenerate modes," *IEEE Trans. Microwave Theory and Techniques*, Vol. 58, No. 12, 3427–3432, 2010.
2. Wang, J., L. Ge, K. Wang, et al., "Compact microstrip dual-mode dual-band bandpass filter with wide stopband," *Electronics Letters*, Vol. 47, No. 4, 263–265, 2011.
3. Lee, C.-H., C.-I. G. Hsu, H.-H. Chen, and Y.-S. Lin, "Balanced single- and dual-band BPFs using ring resonators," *Progress In Electromagnetics Research*, Vol. 116, 333–346, 2011.
4. Chen, C.-Y. and C.-C. Lin, "The design and fabrication of a highly compact microstrip dual-band bandpass filter," *Progress In Electromagnetics Research*, Vol. 112, 299–307, 2011.
5. Yang, R.-Y., H. Kuan, C.-Y. Hung, and C.-S. Ye, "Design of dual-band bandpass filters using a dual feeding structure and embedded uniform impedance resonators," *Progress In Electromagnetics Research*, Vol. 105, 93–102, 2010.
6. Sun, X. and E. L. Tan, "A novel dual-band bandpass filter using generalized trisection stepped impedance resonator with improved out-of-band performance," *Progress In Electromagnetics Research Letters*, Vol. 21, 31–40, 2011.
7. Zhou, L., S. Liu, H. Zhang, X.-K. Kong, and Y.-N. Guo, "Compact dual-band bandpass filter using improved split ring

- resonators based on stepped impedance resonator,” *Progress In Electromagnetics Research Letters*, Vol. 23, 57–63, 2011.
8. Chu, Q. X. and X. M. Lin, “Advanced triple-band bandpass filter using tri-section SIR,” *Electronics Letters*, Vol. 44, 295–296, 2008.
 9. Lai, X., B. Wu, T. Su, and C.-H. Liang, “A novel tri-band filter using stub-loaded open loop ring resonators,” *Microwave and Optical Technology Letters*, Vol. 52, No. 3, 523–526, 2010.
 10. Lai, X., C.-H. Liang, H. Di, and B. Wu, “Design of tri-band filter based on stub loaded resonator and DGS resonator,” *IEEE Microwave and Wireless Components Letters*, Vol. 20, No. 5, 265–267, 2010.
 11. Yang, C.-F., Y.-C. Chen, C.-Y. Kung, J.-J. Lin, and T.-P. Sun, “Design and fabrication of a compact quad-band bandpass filter using two different parallel positioned resonators,” *Progress In Electromagnetics Research*, Vol. 115, 159–172, 2011.
 12. Chen, C.-F., T.-Y. Huang, and R.-B. Wu, “Design of dual- and triple-passband filters using alternately cascaded multiband resonators,” *IEEE Trans. Microwave Theory and Techniques*, Vol. 54, No. 9, 3550–3558, 2006.
 13. Makimoto, M. and S. Yamashita, *Microwave Resonators and Filters for Wireless Communication — Theory, Design and Application*, Springer, New York, 2001.